DOI: 10.1002/ejic.200800507

Ligation of Bipyridyl Ligands to Metal 8-Hydroxyquinolinates – Synthesis, Crystal Structures, and TDDFT Study

Fan Yue,[a,b] Ai-Xin Zhu,[a] Shao-Liang Zheng,*[c] and Xiao-Ming Chen*[a]

Keywords: Bipyridyl ligands / Metal 8-hydroxyquinolinates / Interfaces / TDDFT / X-ray diffraction

Binding of four bipyridyl ligands, 2,2′-bipyridine (L1), 1,10-phenanthroline (L2), 1,4,8,9-tetraazatriphenylene (L3), and dipyrido[3,2-*a*:2′,3′-*c*]phenazine (L4) with Cdq_2/Znq_2 complexes (q = 8-hydroxyquinoline) gave four neutral, mononuclear Cd^{II}/Zn^{II} complexes, namely $[Cdq_2L1]\cdot H_2O\cdot CH_3OH$ (**1**), $[Cdq_2L3]\cdot 3H_2O$ (**2**), $[Cdq_2L4]\cdot 2H_2O$ (**3**), and $[Znq_2L4]\cdot 2CH_3OH$ (**4**). These mixed-ligand compounds were taken as models for investigating the interfacial effect at the electron-transfer layer/light-emitting layer junction in OLEDs by combination of X-ray diffraction, fluorophotometric titration, cyclic voltammetry, and time-dependent density functional theory (TDDFT) calculations. The results shows the formation of these compounds is favorable to energy transition on the contact surface.

Introduction

Developing organic light-emitting devices (OLEDs) is currently a hot topic in scientific research. As a key technology used in OLEDs, multi-layered assembly with inherent contact surface phenomenon has a significant influence on OLED performance. Stable contacts with low interface resistance are required for long-term stability and high power throughput of devices. This can be achieved by removal of the interface energy offsets that hinder carrier motion,[1] or by tight bonding of two layers.[2] The study of interfacial effects to understand internal physical processes is, therefore, very significant for OLED performance.

Polypyridyl compounds are useful molecular units for electronic transmission materials, which may be ascribed to their rigid planar structure with the extended π-electron providing a high electronic fluidity and high electron affinity value (3.8 eV).[3,4] Meanwhile, metal 8-hydroxyquinoline chelates have attracted significant attention as useful light-emitting materials for OLEDs.[5–11] Consequently, the structure-device property correlation of Znq_2 (q = 8-hydroxyquinoline) has been widely reported.[12–16] A discussion of the interfacial effect of polypyridyl compounds and metal 8-hydroyxquinoline chelates (Mq_n) in view of their chemistry is presented in this paper.

To understand the interfacial effect at the electron-transfer layer/light-emitting layer interface, we adopted four bipyridyl ligands as co-ligands to react with Znq_2/Cdq_2 complexes, and constructed four neutral, monomeric Cd^{II}/Zn^{II} complexes, namely $[Cdq_2L1]\cdot H_2O\cdot CH_3OH$ (**1**) (L1 = 2,2′-bipyridine), $[Cdq_2L3]\cdot 3H_2O$ (**2**) (L3 = 1,4,8,9-tetraazatriphenylene), $[Cdq_2L4]\cdot 2H_2O$ (**3**), and $[Znq_2L4]\cdot 2CH_3OH$ (**4**) (L4 = dipyrido[3,2-*a*:2′,3′-*c*]phenazine), which have been structurally characterized (Scheme 1). The electronic transition variations in the presence of the bipyridyl ligands have been studied by means of time-dependent density functional theory (TDDFT) calculations and cyclic voltammetry (CV). The binding stability of bipyridyl ligands to Mq_2 is also studied by fluorophotometric titration.

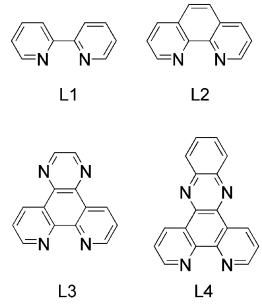

Scheme 1. Structures of the bipyridyl ligands.

Results and Discussion

Crystal Structures

The crystal structures of **1**–**4** revealed that these four neutral complexes all have similar mononuclear structures with

[a] MOE Laboratory of Bioinorganic and Synthetic Chemistry/ State Key Laboratory of Optoelectronic Materials and Technologies, School of Chemistry & Chemical Engineering, Sun Yat-Sen University,
Guangzhou 510275, China
E-mail: cxm@mail.sysu.edu.cn
[b] Chemistry and Chemical Engineering College, Xinjiang University,
Urumqi 830046, China
[c] Department of Chemistry, State University of New York at Buffalo,
Buffalo, New York 14260-3000, USA
Supporting information for this article is available on the WWW under http://www.eurjic.org/ or from the author.

each metal ion being octahedrally coordinated by two deprotonated quinolinolate ligands and a bipyridyl ligand (Figure 1, Table 1). The dihedral angles between two quinolinolate planes are ca. 87.8° in **1**, 87.0° in **2**, 89.7° in **3**, and 87.2° in **4**, respectively; while the dihedral angles between the bipyridyl ligand and two quinolinolate planes are 74.1° and 71.7° in **1**, 70.2° and 61.1° in **2**, 75.4° and 62.9° in **3**, and 78.1° and 81.9° in **4**, respectively. This shows that the orientations of the bipyridyl and quinolinolate ligands are slightly different. On the other hand, the Zn–O bond lengths of 2.061(2) and 2.057(2) Å in **4**, as well as the Cd–O bond lengths of 2.234(4) to 2.261(3) Å in **1**–**3**, are comparable to those observed in the related Znq_2 and Cdq_2 compounds, respectively.[10,11]

Favorable electron-transport capability is required for OLED materials.[17,18] Intermolecular aromatic π-π interactions are conducive to elevating electron mobility of compounds. In the crystal structures of **1**–**4**, there are offset face-to-face π-π stacking interactions between neighboring bipyridyl ligands (Figure 2). The interplanar distances between two adjacent aromatic groups are 3.40(6) Å for **1**, 3.29(6) Å for **2**, 3.37(7) Å for **3**, and 3.40(3) Å for **4**. Besides the head-to-tail aromatic stacking interactions between the bipyridyl ligands from two neighboring molecules, an intermolecular C–H···O hydrogen bond between a bipyridyl ligand and a quinolinolate is found (for details, see Table 2), giving rise to supramolecular dimeric structures in **1**, **2**, and **4**, as well as a chain structure in **3**.

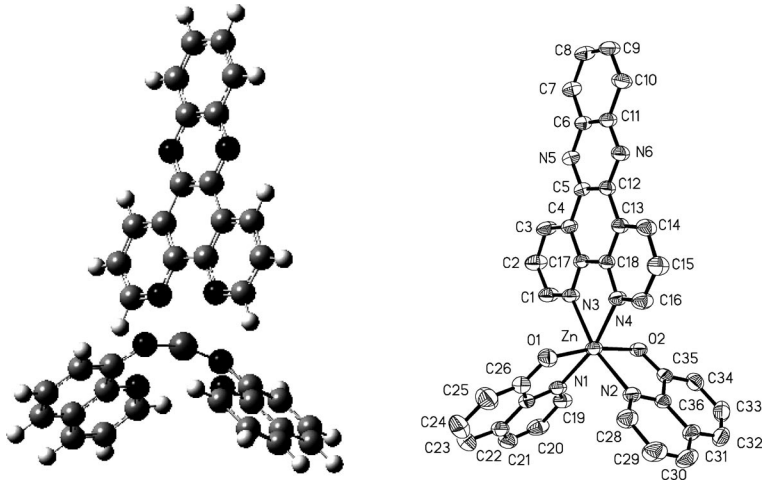

Figure 1. Calculated (left) and crystal (right) structures of **4**.

Table 1. Selected bond lengths [Å] and angles [°].

1					
Cd(1)–O(1)	2.234(4)	Cd(1)–N(1)	2.364(5)	Cd(1)–N(3)	2.348(4)
Cd(1)–O(2)	2.245(4)	Cd(1)–N(2)	2.345(4)	Cd(1)–N(4)	2.335(4)
O(1)–Cd(1)–O(2)	156.6(2)	O(1)–Cd(1)–N(3)	95.6(2)	O(1)–Cd(1)–N(4)	73.0(2)
N(1)–Cd(1)–N(3)	98.9(2)	O(2)–Cd(1)–N(4)	88.9(2)	O(2)–Cd(1)–N(3)	72.9(1)
N(2)–Cd(1)–N(4)	92.8(2)	N(1)–Cd(1)–N(2)	69.3(2)		
2					
Cd(1)–O(1)	2.250(3)	Cd(1)–N(1)	2.349(4)	Cd(1)–N(3)	2.385(4)
Cd(1)–O(2)	2.261(3)	Cd(1)–N(2)	2.330(4)	Cd(1)–N(4)	2.360(4)
O(1)–Cd(1)–O(2)	158.6(1)	O(1)–Cd(1)–N(3)	106.5(1)	O(1)–Cd(1)–N(4)	93.7(1)
N(2)–Cd(1)–N(3)	158.4(1)	O(2)–Cd(1)–N(3)	87.8(1)	O(2)–Cd(1)–N(4)	106.4(1)
N(1)–Cd(1)–N(4)	153.7(1)	N(2)–Cd(1)–N(1)	97.0(1)		
3					
Cd(1)–O(1)	2.233(5)	Cd(1)–N(1)	2.348(5)	Cd(1)–N(3)	2.364(5)
Cd(1)–O(2)	2.233(5)	Cd(1)–N(2)	2.346(5)	Cd(1)–N(4)	2.367(5)
O(2)–Cd(1)–O(1)	156.7(2)	O(1)–Cd(1)–N(3)	103.1(2)	O(1)–Cd(1)–N(4)	95.4(2)
N(3)–Cd(1)–N(2)	156.6(2)	O(2)–Cd(1)–N(4)	106.2(2)	O(2)–Cd(1)–N(3)	92.5(2)
N(1)–Cd(1)–N(4)	160.6(2)	N(2)–Cd(1)–N(1)	100.8(2)		
4					
Zn–O(1)	2.059(2)	Zn–N(1)	2.193(2)	Zn–N(5)	2.155(3)
Zn–O(2)	2.063(2)	Zn–N(2)	2.193(2)	Zn–N(6)	2.156(2)
O(1)–Zn–O(2)	169.86(8)	O(1)–Zn–N(6)	93.6(1)	O(1)–Zn–N(5)	78.8(1)
N(2)–Zn–N(6)	95.63(9)	O(2)–Zn–N(6)	78.7(1)	O(2)–Zn–N(5)	95.1(1)
N(1)–Zn–N(5)	96.03(9)	N(2)–Zn–N(1)	75.01(9)		

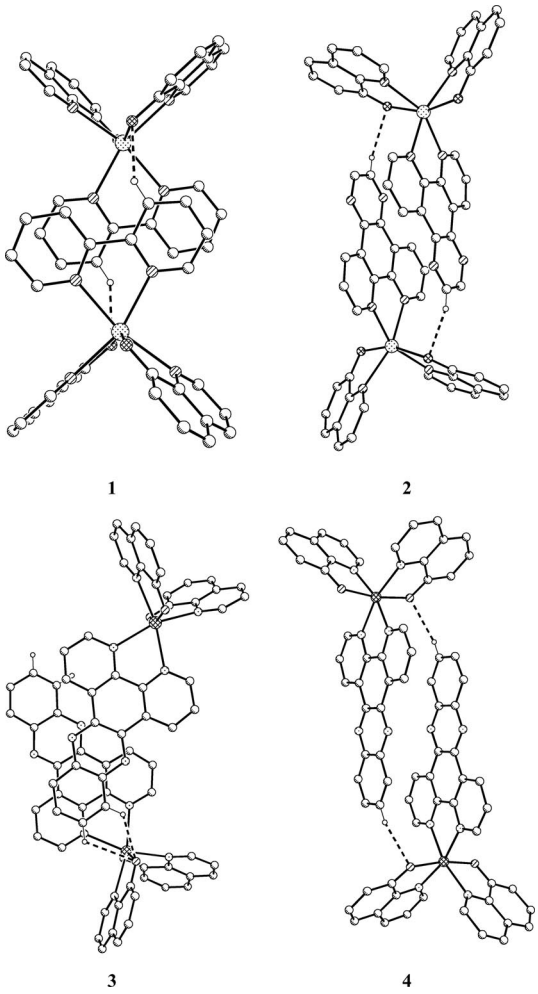

Figure 2. Supramolecular interactions in **1**–**4**.

Table 2. The hydrogen bond lengths [Å] and angles [°].

	D–H···A	*d*(D–H)	*d*(H···A)	*d*(D···A)	<(DHA)
1	C(4)–H(4A)···O(1)#1	0.93	2.65	3.307(8)	128.6
2	C(24)–H(24A)···O(1)#1	0.93	2.63	3.255(6)	125.5
3	C(10)–H(10A)···O(1)#1	0.93	2.79	3.39(2)	123.6
	C(9)–H(9A)···O(1)#1	0.93	3.00	3.51 (2)	116.1
4	C(9)–H(9A)···O(2)#1	0.93	2.51	3.327(4)	147.1

#1 is symmetry code: $-x, -y + 1, -z$ for 1, $-x + 2, -y + 2, -z + 1$ for **2**, $x, -y + 1/2, z + 1/2$ for **3**, and $-x, -y, -z + 2$ for **4**

There are solvent molecules in the crystals, which are involved in the formation of the hydrogen-bonded supramolecular chains. The existence of such solvent molecules leads to the instability of crystals and the deviations between elemental analysis and crystal results.

Theoretical Calculations

Theoretical studies for **4** show that the electron density of the HOMO is concentrated on the phenolato ring, and the LUMO is localized on the bipyridyl ligands (Figure 3), where the strong π-π stacking interactions occur in the crystal structures.

An orbital energy level diagram (Figure 4) for Znq_2, **4**, and L4 was constructed from the calculated orbital eigenvalues for comparison of the variations of HOMO–LUMO energy space upon the introduction of the bipyridyl ligands. Obviously, there is a significant decrease of the energy space from Znq_2 or L4 to the mixed-ligand complex **4**. The calculation results of other complexes are similar to that of **4** (see electronic Supporting Information). When the bipyridyl ligands bind to Zn^{II}, the orientation of two hydroxyquinolinate ligands is changed. The HOMO is contributed by the orbital of the hydroxyquinolinate ligand with higher energy, while the LUMO is contributed by the orbital of the bipyr-

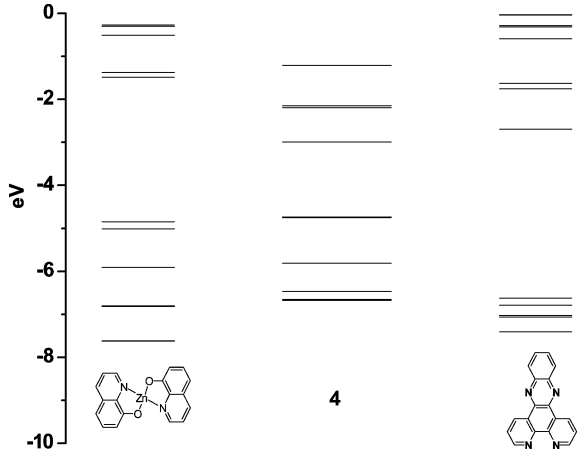

Figure 4. Calculated orbital energy level diagram by B3LYP/6-31++G**.

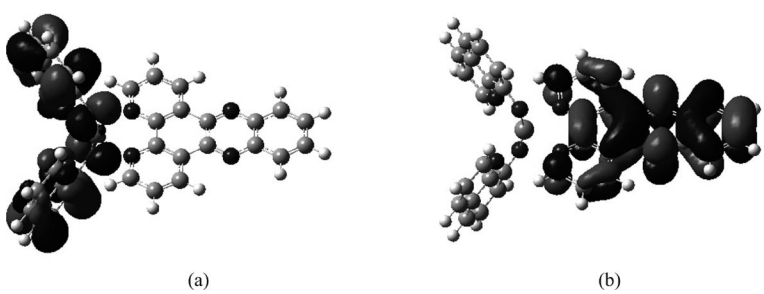

Figure 3. Orbital amplitude plots of the HOMO (a) and LUMO (b) for **4**.

Table 3. Calculated and experimental absorption wavelengths [nm] and transition nature for L4, Znq_2, **4**, Cdq_2, and **3** with oscillator strengths.

Compound	Transition nature	Wavelength		Oscillator strengths	Solvent effect (in MeOH)	Oscillator strengths
		Exp.	Calcd.			
L4	S0–S1	379.0	364.48	0.0065	367.45	0.0099
Znq2	S0–S1	377.0	438.56	0.0947	375.84	0.1223
L4Znq2 (**4**)	S0–S4	376.2	438.14	0.0340	400.16	0.0506
Cdq2	S0–S1	381.0	422.23	0.0533	410.32	0.0652
L4Cdq2 (**3**)	S0–S4	377.2	442.74	0.0503	407.01	0.0539

idyl ligand with lower energy. Consequently, the energy space level in **4** is decreased in comparison to the original complex Znq_2. According to the literature, a stepped decrease of the bandgap can lead to remarkably efficient OLEDs.[1] The calculation result implies that the energy transition in the junction of bipyridyl and Znq_2 layers may be enhanced by the binding of the bipyridyl on the contact surface.

The further results of TDDFT calculations show that the oscillator strengths of mixed-ligand complexes **1**–**4** corresponding to the single-state transition between ground state and excited state are very low (S0–S1 transition: $f = 0.000$). This suggests the luminescence corresponding to the S1–S0 transition is quenched.[19] Actually, when the bipyridyl ligands were added to the solution of Znq2/Cdq2, different fluorescence quenching behaviors were observed. The calculated (Figure 5) and experimental absorption wavelengths (nm) and transition nature are given in Table 3.

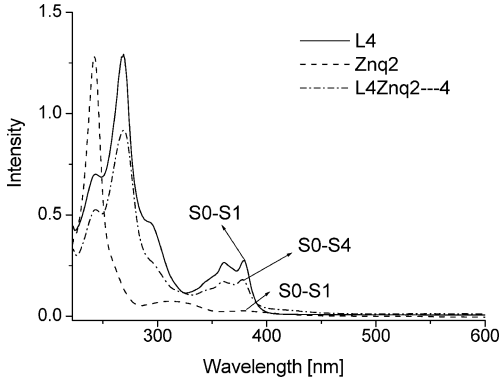

Figure 5. UV/Vis spectra of L4, Znq_2, and $L4Znq_2$ (compound **4**) in MeOH solution (2×10^{-4} mol L^{-1}).

Electrochemical Properties

The cyclic voltammograms of Znq_2 and **4** in acetonitrile show quasi-reversible reduction peaks at –1.12 V and –0.89 V, respectively (Figure 6). According to our previous "gas-state" theoretical calculations, a much lower LUMO energy level is found in **4** (–2.99 eV, while –1.49 eV in Znq_2), which is responsible for its lower reduction potential. The unexpected differences between the electrochemical reduction potentials and calculated results can be attributed to the solvent effect,[20,21] since correction of the solvent effect in calculations leads to the LUMO energy level of –2.66 eV in **4** and –2.21 eV in Znq_2.

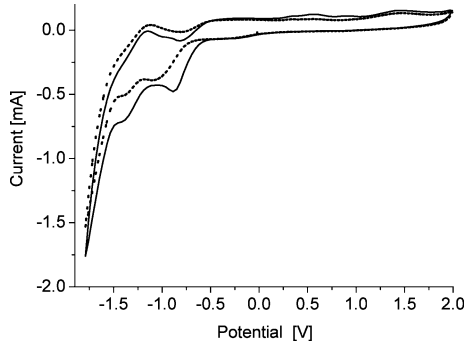

Figure 6. Cyclic voltammograms of Znq_2 (solid line) and **4** (dotted line) measured in MeCN at a scan rate of 200 mV s^{-1}.

Fluorescence Spectra and Titration

The emission spectra of Znq_2/Cdq_2 in CH_3OH display a broad band with a maximum at 546 nm and 542 nm, respectively, assignable to the LLCT.[8] The results of fluorescence titration show that the fluorescence of Znq_2/Cdq_2 was quenched by addition of the bipyridyl ligands. For example, the results of a titration of Cdq_2 by addition of L2 are shown in Figure 7. The fluorescent titration curves were fitted with the nonlinear least-squares curve-fitting method[22] to give the apparent binding constants (K_{app}, M^{-1}) of these mixed-ligand complexes (see Table 4). The constants are around 10^5 M^{-1}, indicating that the binding abilities of bipyridyl ligands to Znq_2/Cdq_2 are fairly strong. These results indicate that the presence of bipyridyl ligands and Znq_2/Cdq_2 at the interface of a device could lead to the binding of bipyridyl ligands to Znq_2/Cdq_2 species, and

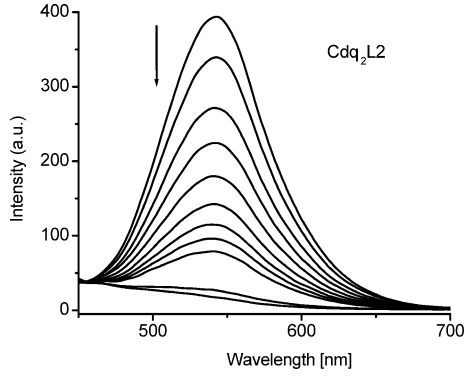

Figure 7. Fluorescent titration spectra of Cdq_2 (20 μM) in MeOH solution upon addition of L2 in MeOH solution. [L2] = 0, 5, 10, 15, 20, 25, 30, 35, 40, 100, 200 μM. λ_{ex} = 389 nm.

consequently to the decrease of luminescence. On the other hand, the binding reaction occurring on the contact surface is advantageous for eliminating delamination between two layers, leading to a more stable combination of two layers.[2]

Table 4. Apparent binding constant K_{app} (10^5 M^{-1}) determined by fluorescence titration (R^2 is coefficient of determination).

Species	K_{app}	R^2	Species	K_{app}	R^2
Znq_2L1	0.182	0.9929	Cdq_2L1	0.148	0.9989
Znq_2L2	1.30	0.9746	Cdq_2L2	1.75	0.9929
Znq_2L3	1.18	0.9965	Cdq_2L3	1.25	0.9958
Znq_2L4	2.26	0.9976	Cdq_2L4	2.11	0.9992

Conclusions

This work demonstrates that the bipyridyl ligands can strongly bind to Cd^{II}/Zn^{II} bis-quinolinolate complexes, furnishing neutral, stable, mononuclear mixed-ligand Cd^{II}/Zn^{II} complexes. Such binding interactions may occur in the interface of multi-layered OLEDs. According to our investigation of the Cd^{II}/Zn^{II} bis-quinolinolates with the bipyridyls as co-ligands, the HOMO–LUMO energy space level can be tuned with an energy decrease of the LUMO upon ligation of the bipyridyl ligands to Cd^{II}/Zn^{II} complexes, which switches the location of LUMO orbitals to the bipyridyl ligand. Such a change causes fluorescent quenching due to the low oscillator strength corresponding to an intramolecular inter-ligand S_0–S_1 transition. Furthermore, as shown in the crystal structures, the bipyridyl ligands can involve strong π-π stacking interactions in the solid state. Therefore, when binding bipyridyl ligands to Cd^{II}/Zn^{II} bis-quinolinolate complexes at the interface of multi-layered OLEDs, a shortening of the intermolecular distance for electron transport occurs, thus the electron transport will be enhanced at the interface.

Experimental Section

Materials and Measurements: All of the starting chemicals were of analytical reagent grade. L3 and L4 were synthesized according to a literature procedure.[23] Compounds **1**–**4** were synthesized through conventional solution methods using the starting reagents in the stoichiometries of the corresponding products.

The C, H, and N microanalyses were carried out with an Elementar Vario E1 Elemental analyzer. The steady-state fluorescence spectra were determined with a Shimadzu RF-5301pc spectrofluoro-photometer.

The cyclic voltammetry measurements were performed with a dried acetonitrile solution (10^{-4} M) containing tetrabutylammonium perchlorate (0.1 M) as the supporting electrolyte, a three-electrode set up employed a Pt working electrode, a Pt counter electrode, and Ag/AgCl/KCl(satd.) as the reference electrode. The electrochemical measurements were recorded at a scan rate of 200 mV s^{-1}.

Theoretical Calculations: TDDFT calculations were performed at the B3LYP level with a 6-31++G** basis set, and the LanL2DZ set with an effective core potential for metal, by employing the Gaussian03 suite of programs.[24] Starting with the X-ray geometries, the structures were optimized by energy minimization. The Mq_2 structure was employed directly from reported crystal structure.[11,13] The electron-density diagrams of molecular orbitals were obtained with the Gaussview graphics program.

Synthesis and Characterization

[Cdq_2L1]·H_2O·CH_3OH (1): To an ethanol solution (30 mL) of L1 (0.18 g, 1 mmol) at room temperature was added $Cd(OAc)_2·2H_2O$ (0.266 g, 1 mmol), and whilst stirring HQ (2 mmol) was slowly added to the mixture. A yellow precipitate was formed. Then CH_3Cl (30 mL) and MeOH (10 mL) were added to the mixture, the precipitate was filtered off, and the filtrate was transferred to several tubes. The colorless crystals for X-ray work were grown by very slow evaporation of the mixture solution for ca. 2 months. After washing with ethanol, the product was collected in 30% yield (0.19 g). $C_{29}H_{22}CdN_4O_4$ (602.92): calcd. C 57.77, H 3.68, N 9.29; found C 58.50, H 3.57, N 9.48.

[Cdq_2L3]·$3H_2O$ (2): The pale-yellow crystals of **2** were obtained as for **1** by using L3 instead of L1. Pale-yellow block crystals of **2** were obtained for about 20 days in 25% yield (0.17 g). $C_{32}H_{26}CdN_6O_5$ (687.01): calcd. C 55.95, H 3.81, N 12.23; found C 57.45, H 3.76, N 12.56.

[Cdq_2L4]·$2H_2O$ (3): Complex **3** was prepared as for **1** by using L4 instead of L1. Yellow crystals of **3** were obtained for 3–5 days in 70% yield (0.54 g). $C_{36}H_{26}CdN_6O_4$ (719.04): calcd. C 60.13, H 3.64, N 11.69; found C 61.09, H 3.98, N 11.25.

[Znq_2L4]·$2CH_3OH$ (4): Complex **4** was prepared as for **1**. Pale-yellow crystals of **4** were obtained for 5–7 days. The yield was 0.44 g (60%). $C_{36}H_{26}N_6O_4Zn$ (672.02): calcd. C 64.34, H 3.90, N 12.51; found C 63.79, H 4.099, N 12.27.

Crystallographic Studies: The single-crystal diffraction data were collected with a Bruker Smart Apex CCD diffractometer with graphite-monochromated Mo-K_α radiation (λ = 0.71073 Å) at room temperature, and the absorption corrections were applied by SADABS. The structures were solved by direct methods and refined using a full-matrix least-squares technique with SHELXL.[25] All non-hydrogen atoms were refined with anisotropic displacement parameters, whereas the organic hydrogen atoms were placed at idealized positions and refined as riding atoms. Experimental details of the X-ray analyses are provided in Table S1. Selected bond lengths and angles are listed in Table 1.

CCDC-651184 (for **1**), -651185 (for **2**), -651186 (for **3**), and -651187 (for **4**) contain the supplementary crystallographic data for this paper. These data can be obtained free of charge from the Cambridge Crystallographic Data Centre via www.ccdc.cam.ac.uk/datarequest/cif.

Supporting Information (see also the footnote on the first page of this article): Calculation results for Znq2, L2 to L4 and complexes **1**–**3**. Fluorescent titration spectra of Znq2/Cdq2 solutions and upon addition of bipyridyl ligands. Nonlinear least-squares curve-fitting results of fluorescent titration. Summary of crystallographic data.

Acknowledgments

This work was supported by the Ministry of Science and Technology of China (2007CB815302), the University of Hong Kong, Nano and Advanced Materials Institute Limited and Innovation and Technology Commission of the Hong Kong Special Administrative Region, China (ITS/016/08NP) and Science and Technology Department of Guangdong Province (No. 04205405).

[1] P. K. H. Ho, J. S. Kim, J. H. Burroughes, H. Becker, S. F. Y. Li, T. M. Brown, F. Cacialli, R. H. Friend, *Nature* **2000**, *404*, 481–484.
[2] Y. Q. Zhan, Z. H. Xiong, H. Z. Shi, S. T. Zhang, Z. Xu, G. Y. Zhong, J. He, J. M. Zhao, Z. J. Wang, E. Obbard, H. J. Ding, X. J. Wang, X. M. Ding, W. Huang, X. Y. Hou, *Appl. Phys. Lett.* **2003**, *83*, 1656–1658.
[3] S. Naka, H. Okada, H. Onnagawa, T. Tsutsui, *Appl. Phys. Lett.* **2000**, *76*, 197–199.
[4] M. A. Baldo, S. Lamansky, P. E. Burrows, M. E. Thompson, P. E. Forrest, *Appl. Phys. Lett.* **1999**, *75*, 4–6.
[5] C. W. Tang, S. A. VanSlyke, *Appl. Phys. Lett.* **1987**, *51*, 913–915.
[6] P. E. Burrows, L. S. Sapochak, D. M. McCarty, S. R. Forrest, M. E. Thompson, *Appl. Phys. Lett.* **1994**, *64*, 2718–2720.
[7] P. E. Burrows, Z. Shen, V. Bulovic, D. M. McCarty, S. R. Forrest, J. A. Cronin, M. E. Thompson, *J. Appl. Phys.* **1996**, *79*, 7991–8006.
[8] B. C. Lin, C. P. Cheng, Z.-Q. You, C.-P. Hsu, *J. Am. Chem. Soc.* **2005**, *127*, 66–67.
[9] a) R. Pohl, V. A. Montes, J. Shinar, P. Anzenbacher Jr, *J. Org. Chem.* **2004**, *69*, 1723–1725; b) R. Pohl, P. Anzenbacher Jr, *Org. Lett.* **2003**, *5*, 2769–2772.
[10] K. S. Yang, H. K. Shin, C. Kim, Y. S. Kwon, *Synth. Met.* **2005**, *12*, 245–248.
[11] L. S. Sapochak, F. E. Benincasa, R. S. Schofield, J. L. Baker, K. K. C. Riccio, D. Fogarty, H. Kohlmann, K. F. Ferris, P. E. Burrows, *J. Am. Chem. Soc.* **2002**, *124*, 6119–6125.
[12] B.-S. Xu, Y.-Y. Hao, H. Wang, H.-F. Zhou, X.-G. Liu, M.-W. Chen, *Solid State Commun.* **2005**, *136*, 318–322.
[13] L. L. Merritt, R. T. Cady, B. W. Mundy, *Acta Crystallogr.* **1954**, *7*, 473–476.
[14] K. Yasushi, M. Masahiro, Y. Noritake, K. Nobutami, *Bull. Chem. Soc. Jpn.* **1985**, *58*, 1631–1635.
[15] N. Donzé, P. Péchy, M. Grätzel, M. Schaer, L. Zuppiroli, *Chem. Phys. Lett.* **1999**, *315*, 405–410.
[16] M. Uchida, J. Izumisawa, M. Uchino, K. Furukawa, *JP Patent* No. 06145146, **1994**.
[17] A. P. Kulkarni, C. J. Tonzola, A. Babel, S. A. Jenekhe, *Chem. Mater.* **2004**, *16*, 4556–4573.
[18] G. Hughes, M. R. Bryce, *J. Mater. Chem.* **2005**, *15*, 94–107.
[19] S.-L. Zheng, P. Coppens, *Cryst. Growth Des.* **2005**, *5*, 2050–2059.
[20] S. Fantacci, F. De Angelis, A. Selloni, *J. Am. Chem. Soc.* **2003**, *125*, 4381–4387.
[21] S. Fantacci, F. De Angelis, A. Sgamellotti, N. Re, *Chem. Phys. Lett.* **2004**, *396*, 43–48.
[22] Y. Liu, B. Li, B.-H. Han, T. Wada, Y. Inoue, *J. Chem. Soc. Perkin Trans. 2* **1999**, *2*, 563–568.
[23] J. Bolger, A. Gourdon, E. Ishow, J.-P. Launay, *Inorg. Chem.* **1996**, *35*, 2937–2944.
[24] M. J. Frisch, G. W. Trucks, H. B. Schlegel, G. E. Scuseria, M. A. Robb, J. R. Cheeseman, J. A. Montgomery Jr, T. Vreven, K. N. Kudin, J. C. Burant, J. M. Millam, S. S. Iyengar, J. Tomasi, V. Barone, B. Mennucci, M. Cossi, G. Scalmani, N. Rega, G. A. Petersson, H. Nakatsuji, M. Hada, M. Ehara, K. Toyota, R. Fukuda, J. Hasegawa, M. Ishida, T. Nakajima, Y. Honda, O. Kitao, H. Nakai, M. Klene, X. Li, J. E. Knox, H. P. Hratchian, J. B. Cross, C. Adamo, J. Jaramillo, R. Gomperts, R. E. Stratmann, O. Yazyev, A. J. Austin, R. Cammi, C. Pomelli, J. W. Ochterski, P. Y. Ayala, K. Morokuma, G. A. Voth, P. Salvador, J. J. Dannenberg, V. G. Zakrzewski, S. Dapprich, A. D. Daniels, M. C. Strain, O. Farkas, D. K. Malick, A. D. Rabuck, K. Raghavachari, J. B. Foresman, J. V. Ortiz, Q. Cui, A. G. Baboul, S. Clifford, J. Cioslowski, B. B. Stefanov, G. Liu, A. Liashenko, P. Piskorz, I. Komaromi, R. L. Martin, D. J. Fox, T. Keith, M. A. Al-Laham, C. Y. Peng, A. Nanayakkara, M. Challacombe, P. M. W. Gill, B. Johnson, W. Chen, M. W. Wong, C. Gonzalez, and J. A. Pople, *Gaussian 03*, Revision B.03, Gaussian, Inc., Pittsburgh PA, **2003**.
[25] G. M. Sheldrick, *SHELXL-97*, Program for X-ray Crystal Structure Solution, Göttingen University, Germany, **1997**.

Received: May 22, 2008
Published Online: October 10, 2008

